

Voltage-controlled precision electronic power regulator

Cite as: Rev. Sci. Instrum. 92, 124708 (2021); doi: 10.1063/5.0071683

Submitted: 16 September 2021 • Accepted: 2 December 2021 •

Published Online: 20 December 2021



View Online



Export Citation



CrossMark

S. B. Rutin^{a)} 

AFFILIATIONS

Institute of Thermal Physics, Ural Branch, Russian Academy of Sciences, Amundsena St. 107a, Ekaterinburg 620016, Russian Federation

^{a)}Author to whom correspondence should be addressed: ryutin.sergey@gmail.com

ABSTRACT

The architecture of a novel electronic power regulator, which allows a set value of constant power on a wire probe to be maintained, is presented. A gain in the negative feedback loop of $\approx 2 \cdot 10^3$ allows the set power value in the series of pulses to be accurately maintained at the level of 99.95% (proximity 0.05). In order to study short term processes, the response time of the described regulator is in the order of $2 \mu\text{s}$. The created architecture is easily scalable for various tasks, ranging from the well-known transient hot-wire method to other applications, examples of which are given in this article (unsteady heat transfer in supercritical-pressure fluids and unstable mixtures having lower critical solution temperature). A comparison of the presented controller architecture with the previously described solutions from the point of view of operational stability is given.

Published under an exclusive license by AIP Publishing. <https://doi.org/10.1063/5.0071683>

INTRODUCTION

The creation of a regulator that allows a sufficiently accurate set power value to be maintained on a heater is not as simple as might at first glance seem. Such a regulator is especially in demand in the implementation of the THW (transient hot-wire) method for measuring thermal conductivity,^{1–3} since the requirement for a constant heat flux from the wire heater can only be realized by ensuring the constancy of the electrical power dissipated on the heater.⁴ The task of maintaining constant power is complicated by the changes occurring in the resistance of the heater along with an increase in its temperature during heating. Previous attempts to create such a regulator had to be abandoned due to the instability of the existing regulator models.^{5,6} The complexity of the problem is due to the fact that the controller is two-dimensional (two input values) and nonlinear (multiplication of input values), while the control object (heater-probe) is essentially nonstationary since the resistance of the probe changes during heating. In addition, the probe has its own thermal relaxation time, which depends on its geometric parameters as well as the material and thermo-physical properties of the medium in which it is immersed. All of the above makes the task of modeling such a device by means of the standard automatic control theory practically impossible. For this reason, the correct selection of circuit architecture in order to achieve a stable operation of the regulator can be made based

on the accumulated experience, taking into account the designer's intuition.

ARCHITECTURE

The discussion of the question of architecture begins with the description presented in Ref. 5. Figure 1 shows the equivalent architecture from this article.

The functional appearance of the architecture is concomitant with reality since the data on thermal conductivity presented in Ref. 5 were obtained with the help of this implementation. However, in Ref. 6, the same authors reported the following: "Another practical problem with the previous system was the dynamical behavior of the feedback circuit, which involved an analog multiplier in order to provide constant power during the pulse. It was not easy to obtain stable operation as well as short rise time over a wide range of load currents. The AID converter previously used had an effective sampling time of only a few μs , which made it quite sensitive to interfering spikes. In summary, we found it desirable to simplify the circuitry as much as possible, making use of the best instruments commercially available at the present time." From the passage quoted above, it is clear that the authors abandoned the use of the device they had created due to its inability to cope with the problem of instability.

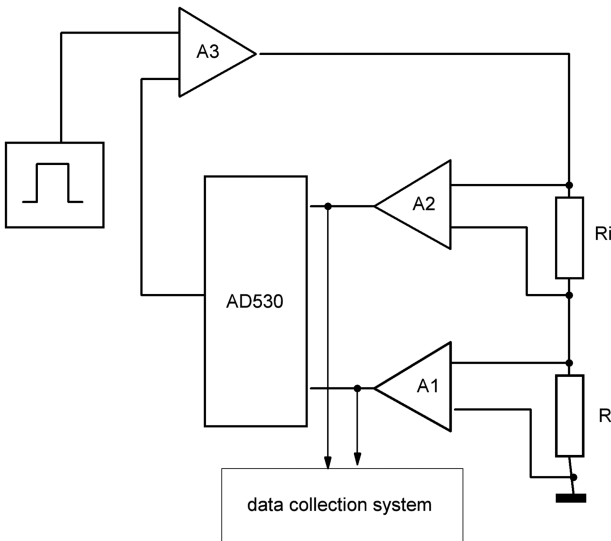


FIG. 1. Schematic architecture of the constant power generator presented in Ref. 5: A1—buffer amplifier of a signal from a current-measuring resistor R_i ; A2—buffer amplifier of a signal from a R probe; AD530—multiplier of analog signals; and A3—unit for comparing the control voltage from a pulse generator with a signal at the output of the multiplier, which is used to maintain a zero difference between them, the output of which feeds the R_i —R circuit, thereby maintaining a constant power at the R probe.

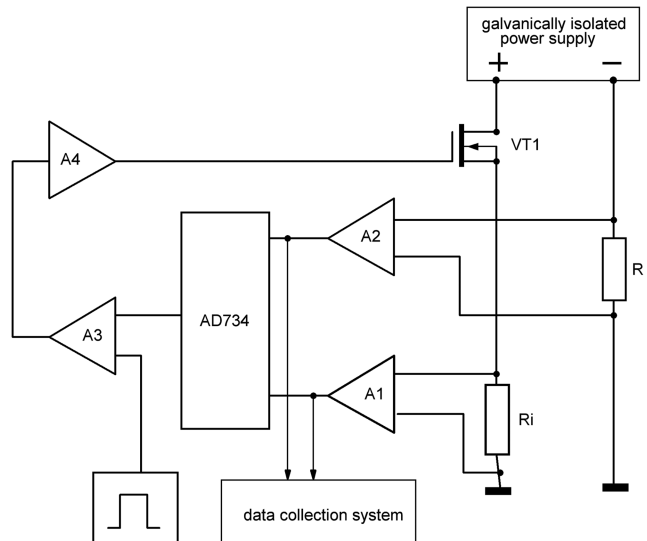


FIG. 2. Constant power generator providing a stable operation across a wide range of load currents: A1—buffer amplifier of a signal from a current-measuring resistor R_i ; A2—buffer amplifier of a signal from a probe R; AD734—analog multiplier; A3—node for comparing the control voltage from a pulse generator with a signal at the output of the multiplier to maintain a zero difference between them; and A4—amplifier whose output signal controls the power element VT1. The circuit has a galvanically isolated power supply for the R_i —R circuit.

The main reason for the instability in this case lies in the imperfection of the electronic components used, namely, the buffer amplifiers A1 and A2. Irrespective of what kind of operational or instrumentation amplifiers are used, the common mode rejection ratio (CMRR) remains a finite value, which tends to decrease rapidly with increasing frequency. Since R and R_i are in series connection, the inevitably strong mutual influence of A1 on A2 prevents the stable operation of the device. In addition, the rather large gain coefficient ($\approx 10^3$) required in the negative feedback loop to obtain the desired control accuracy exacerbates the problem of mutual influence.

A clue to a possible solution for indicating the optimal circuit architecture is contained in Ref. 7, which describes an approach to creating a current generator with a grounded load. By applying this idea to a power control device, it was possible to arrive at a general architecture, as shown in Fig. 2.

This galvanically isolated power supply architecture provides a common ground phase in the circuit on which all the feedback loop components as well as the current-measuring resistor and the probe rely, significantly reducing the problem of the CMRR final value. It is no coincidence that it is the current-measuring resistor that is connected to the source of VT1 since in this case VT1 operates in the mode of a current generator to provide additional stability to the entire circuit. If the probe and the resistor positions are swapped around, the stability of the regulator is significantly reduced.

In order to clarify the important nuances, let us turn to the simplified schematic diagram of the regulator shown in Fig. 3. An example of calculating the nominal values of elements for scaling voltage levels in the regulator is presented in the Appendix.

Some important features should be noted:

- All the operational amplifiers, A1, A2, A3, and A4, are in inverting connection. This means that in operating mode, quasi-zero is maintained at the inverting input of each of them; moreover, both inputs of each op-amp are connected to the ground phase.
- A1 and A2 must be selected with the unity-gain stable option (e.g., LF356) since the gains of these units can be equal to or less than one, depending on the parameters of the probe used. Due to the voltage of the AD734 multiplier input window being 10 V, proper scaling of the voltage drops across the current-measuring resistor R_i and the probe R is required to fit into the multiplier input window.
- Resistors R8 and R9 directly connected to R_i and R must satisfy the conditions $R_8 \gg R_i$ and $R_9 \gg R$ in order not to significantly affect the operation of the “probe/current-measuring resistor” circuit.
- The response time of the controller is determined from the relation $\tau = R_1 \cdot C_1$. C_1 is selected in the process of setting up the entire circuit based on the minimum value at which the operation of the circuit is stable. When using such LF356 operational amplifiers as represented by A1–A4, it is possible to obtain a response time of the order of $2 \mu\text{s}$.
- The required accuracy of maintaining a given power level is provided by a large gain in the negative feedback loop. For example, if the transmission coefficients A1 and A2 are of the order of one, then the transmission coefficient of A3 can be set to 10, while the transmission coefficient of A4 can be

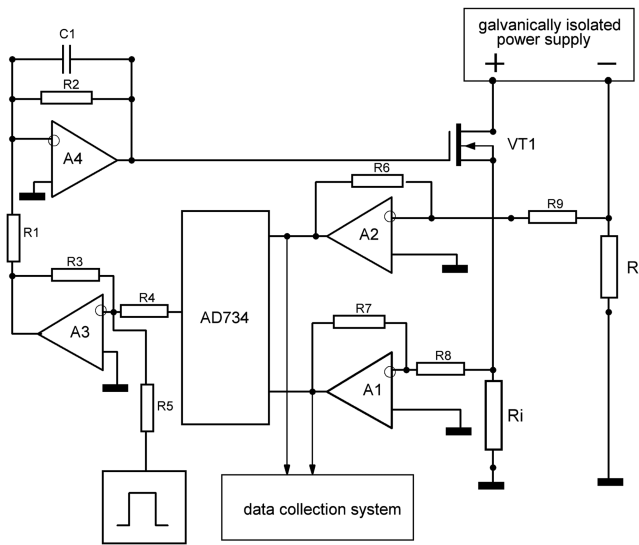


FIG. 3. Simplified schematic diagram of a regulator that ensures the constancy of electrical power dissipated on a heater (probe R). Here, R_i —precise current-measuring resistor; A1—voltage drop buffer amplifier across a current-measuring resistor R_i ; A2—buffer amplifier for a voltage drop across the heater (probe R); AD734—analog multiplier; A3—unit for comparing the control voltage from the pulse generator with the signal at the output of the multiplier in order to maintain a zero difference between them; A4—integrator, whose output controls the power element VT1; and VT1—power MOSFET IRF540Z. The diagram does not display the elements of protection against emergency modes as well as the galvanic isolation of power supply circuits.

set to 200. In this case, the total transmission coefficient of $\approx 2 \times 10^3$ will ensure that the power value is maintained to the required accuracy.

- In order to maintain the set power value in the pulse train at the level of 99.95%, the source of the control pulse voltage must be of appropriate quality; for example, it can be generated by a 16-bit DAC. In this case, the regulator will correspond to the class of 0.05 to ensure the execution of the algorithm $P_{\text{out}} = k \cdot U_{\text{in}}$, where P_{out} is the set power value, U_{in} is the input control voltage, and k is a constant factor.

Separately, we note that the use of an op-amp in a non-inverting connection in this architecture does not allow a stable operation of the regulator to be achieved. Here, it might seem that non-inverting switching would be much more effective since in this case, the input resistance of the op-amp in the order of tens of megohms does not exert any influence on the “probe/current-measuring resistor” circuit. However, practical experience has shown that it is not possible to achieve a stable operation of the regulator in this case.

APPLICATION

On the basis of the above-described regulator, an experimental setup was created, comprising a hardware-software complex controlled by a specially written software shell. During the experiments carried out on supercritical heat transfer at heating times varying between units and tens of milliseconds, the effect of a threshold decrease in the intensity of heat transfer when passing through the critical temperature region was identified.^{8–11} Figure 4 shows an example of such a critical transition.

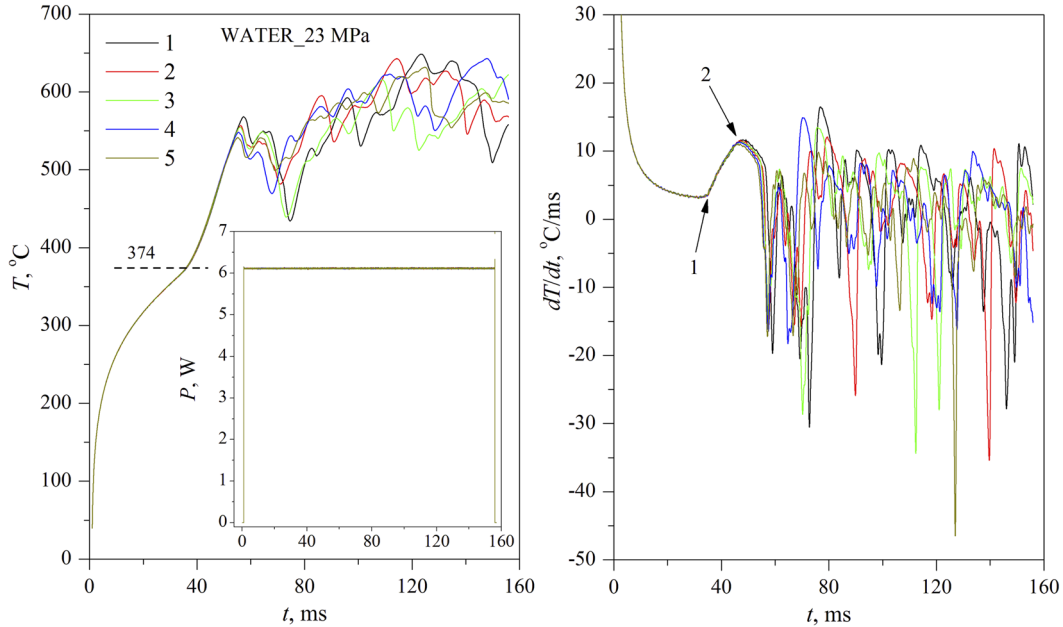


FIG. 4. Heating the probe in water pre-compressed to 23 MPa. The probe comprises a platinum wire with a diameter of 20 μm and a length of 1 cm. The thermograms $[T(t)]$ are shown on the left, the critical temperature is indicated by the dashed line, while the numbers correspond to the pulse number at the same set power. The time derivatives of the thermograms are shown on the right. The inset on the left shows the power $P(t)$ for all five pulses in raw format. The heat flux density amounts to $\approx 8.9 \text{ mW/m}^2$.

Figure 4 shows that the thermograms deviate sharply upward in the course of passing the region of a substance critical temperature, indicating a threshold decrease in the intensity of heat transfer. Since the power value was maintained in a series of pulses at an accuracy of 99.95%, the thermograms prior to the onset of gravitational convection are almost identical. The threshold character of the critical transition indicated by arrow number 1 can be clearly seen in the graph of derivatives. Arrow number 2 marks the beginning of the gravitational convection. For more details, see Refs. 8–11.

The same experimental approach was used to study unsteady heat transfer in solutions having a lower critical solution temperature (LCST). For example, for the solution polypropylene glycol PPG-425/water, the spinodal decomposition of the solution was found upon deep penetration into the region of instability.^{12,13} Here, the manifestation of spinodal decomposition was expressed in a significant intensification of heat transfer when thermograms from a certain temperature value take an almost horizontal form while absorbing high heat flux densities. Figure 5 shows the thermograms for a PPG-425/water solution having a volume concentration of 30%. They demonstrate a nearly horizontal aspect in the temperature range 240–260 °C while absorbing a heat flux density of the order of 9.4 MW/m². This is quite unusual for individual liquids and solutions having unlimited solubility. For more details, see Refs. 12 and 13.

The method was also applied to measure the thermal conductivity coefficient. Here, the THW-method used was based on the classical version,^{14,15} which assumes the action of an infinite linear heat source that generates a constant heat flux density. Here, if a wire probe of finite length is used due to the impossibility of creating an infinite linear source, then it is quite feasible to ensure a constant heat flux density by maintaining constant power. It is shown in Ref. 4 that the use of direct current in the THW-method leads to

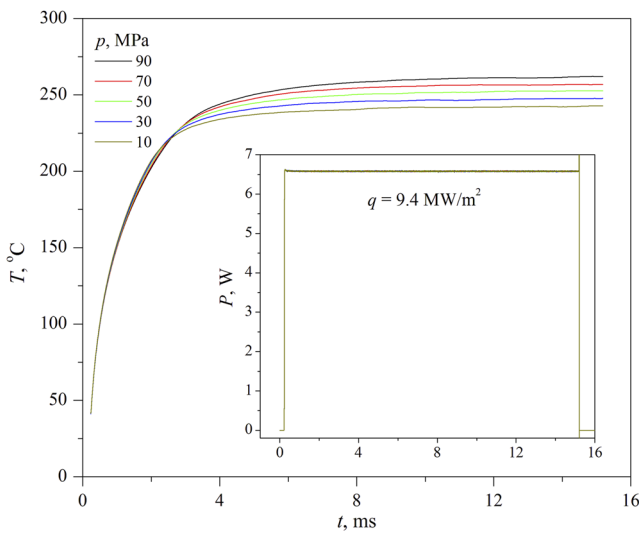


FIG. 5. Thermograms of probe heating in a PPG-425/water solution along the isobars. The probe comprises a platinum wire having a diameter of 20 μm and a length of 1.1 cm. The volumetric concentration of PPG is 30%. The inset shows the power plots superimposed on each other for all five pulses. It also shows a calculated estimate of the heat flux density.

a significant uncertainty in the obtained thermal conductivity coefficient values, which have a strong dependence on the diameter of the probe. Accordingly, existing commercial installations use rather sophisticated techniques to reduce this uncertainty. However, the approach we propose here allows the uncertainty associated with the use of direct current to be eliminated; moreover, the final result can be obtained by providing just one pulse.

CONCLUSION

The created controller architecture demonstrated stable operation and convenient scalability for various experimental tasks. From below, the current range is limited only by the noise characteristics of the components used; from above, it is practically unlimited. If more power and the corresponding current are required, a parallel assembly of power MOSFETs can always be used. In the above applications, the operating currents vary from ≈0.1–2.5 A, which cover a heat flux density range of 10 kW/m² to 20 MW/m². If the required performance is higher than the one presented, faster op-amps need to be selected along with an analog multiplier. Thus, the presented controller can be applied to a wide range of experimental problems associated with heating under strictly specified conditions, including exotic problems, such as heat transfer by thermodynamically unstable solutions.

ACKNOWLEDGMENTS

This work was supported by the Russian Science Foundation (Project No. 19-19-00115).

AUTHOR DECLARATIONS

Conflict of Interest

The author declares no conflicts of interest.

DATA AVAILABILITY

The data that support the findings of this study are available from the corresponding author upon reasonable request.

APPENDIX: THE OPERATION OF THE REGULATOR

The operation of the regulator assumes a preliminary adjustment of the scaling of voltage levels at key points of the circuit (see Fig. 3). The multiplier processes input voltages up to 10 V. Accordingly, the choice of the values of the resistors R₆–R₉ should ensure that the level of the output voltages of the buffer amplifiers A₁ and A₂ is no more than 10 V. The transfer function of the multiplier is written as follows: $U_{\text{out}} = (U_{\text{in1}} * U_{\text{in2}})/10$, i.e., the transmission coefficient is conventionally equal to one. On the probes we used (platinum wires with a diameter of 20 μm and a length of 1 cm), the resistance of the probe changes from 3 Ω (room temperature) to ≈9.7 Ω (temperature 700 °C). The voltage drop across the probe in this case exceeds 10 V. In this regard, the transmission coefficient of the amplifier A₂ is chosen to be equal to 0.5. In this case, R₉ = 5 kΩ and R₆ = 10 kΩ. The value of the current-measuring resistor is selected from the condition that the current through the probe does not exceed 2 A. In this case, R_i = 5 Ω. The voltage drop across it does

not exceed 10 V and the transmission coefficient of the amplifier A1 is chosen equal to 1. The values of the resistors R7 and R8 = 10 k Ω . This will automatically scale the rest of the regulator correctly. For other applications, when higher or lower currents and powers are needed, the scaling procedure is done in the same way as presented.

REFERENCES

- ¹M. J. Assael, K. D. Antoniadis, and W. A. Wakeham, *Int. J. Thermophys.* **31**, 1051 (2010).
- ²H. M. Roder, R. A. Perkins, A. Laesecke, and C. A. N. de Castro, "Absolute steady-state thermal conductivity measurements by use of a transient hot-wire system," *J. Res. Natl. Inst. Stand. Technol.* **105**, 221 (2000).
- ³D. Kim, S. Z. S. Al Ghafri, X. Yang, S. K. Mylona, T. J. Hughes, L. McElroy, and E. F. May, *Int. J. Thermophys.* **42**, 164 (2021).
- ⁴U. Hammerschmidt and W. Sabuga, *Int. J. Thermophys.* **21**, 1255 (2000).
- ⁵P. Andersson and G. Backstrom, *Rev. Sci. Instrum.* **47**, 205 (1976).
- ⁶B. Håkansson, P. Andersson, and G. Bäckström, *Rev. Sci. Instrum.* **59**, 2269 (1988).
- ⁷P. Horowitz and W. Hill, *The Art of Electronics*, 2nd ed. (Cambridge University Press, 1989).
- ⁸S. B. Rutin and P. V. Skripov, *Int. J. Heat Mass Transfer* **57**, 126 (2013).
- ⁹S. B. Rutin and P. V. Skripov, *Thermochim. Acta* **562**, 70 (2013).
- ¹⁰S. B. Rutin and P. V. Skripov, *Int. J. Heat Mass Transfer* **79**, 526 (2014).
- ¹¹S. B. Rutin, A. A. Igolnikov, and P. V. Skripov, *J. Eng. Thermophys.* **29**, 67 (2020).
- ¹²A. A. Igolnikov, S. B. Rutin, and P. V. Skripov, *Thermochim. Acta* **695**, 178815 (2021).
- ¹³A. Igolnikov, S. Rutin, and P. Skripov, *Liquids* **1**, 36 (2021).
- ¹⁴S. B. Rutin, D. A. Galkin, and P. V. Skripov, *Appl. Therm. Eng.* **129**, 145 (2018).
- ¹⁵S. B. Rutin, D. A. Galkin, and P. V. Skripov, *Int. J. Heat Mass Transfer* **115**, 769 (2017).